Nonlinear Optical Polymers. 1. Novel Network Polyurethane with Azobenzene Dye in the Main Frame

Naoto Tsutsumi,* Shuji Yoshizaki, Wataru Sakai, and Tsuyoshi Kiyotsukuri

Department of Polymer Science & Engineering, Kyoto Institute of Technology, Matsugasaki, Sakyoku, Kyoto 606, Japan

Received March 13, 1995; Revised Manuscript Received June 27, 1995®

ABSTRACT: Novel nonlinear optical (NLO) network polyurethane of lysine triisocyanate (LTI) with 4-[*N*-(2-hydroxyethyl)-*N*-methylamino]-3′-(hydroxymethyl)azobenzene (AZODIOL) dye as a NLO-phore has been prepared for second harmonic generation (SHG). A soluble prepolymer of LTI with AZODIOL was prepared, and then a thin prepolymer film was spun-cast on an indium tin oxide coated glass substrate. Two types of poling were carried out. One-step poling process: while high voltage between 5.0 and 8.0 kV was applied to the corona wire, the sample film was heated up and held at a temperature range of 70–190 °C for 10 min and then cooled down to room temperature for 40 min. Two-step poling process: while high voltage was applied to the corona wire, the sample was heated up and held at 90 °C for 1 h and then heated up again and held at a temperature range of 90–190 °C for 30 min. Then the sample was cooled down to room temperature while applying the poling field. The effects of the above poling condition and storage time and thermal annealing on SHG activity are investigated in connection with polymer structure. Better long-term thermal stability of SHG at room temperature can be obtained for the sample prepared by a two-step poling process. This better thermal stability is interpreted to be due to the smaller free volume for that sample.

Introduction

Polymeric materials having second harmonic generation (SHG) must be macroscopically noncentrosymmetric. For these materials, electrical poling is a common procedure for breaking the center of symmetry of randomly oriented nonlinear optical (NLO) dye molecules to achieve noncentrosymmetric alignment. The preferential alignment of NLO molecules was perturbed or disoriented by a molecular relaxation of materials, however, even if the sample was kept at a temperature below the glass transition temperature (T_g). Many efforts have been made to suppress the relaxation of NLO molecules in the polymeric matrix, for the purpose of fabricating thermally stable NLO polymeric materials.[1–9] One approach is the use of cross-linking to suppress the segmental molecular motion of polymer matrix.[2,4–6,8,9] Another approach is the utilization of high-T_g material, such as polyimide, for a thermally stable host in a guest–host NLO system.[7]

Recently, we have developed a novel three-dimensional network polyurethane with an azobenzene moiety in the main frame. Soluble polyurethane prepolymer can be prepared from the trifunctional isocyanate monomer and diol monomer with an azobenzene moiety in the main frame. Prepolymer can be spin-coated on a glass substrate, and the following heat treatment at higher elevated temperature gave rise to the cross-linking to form a uniform network.

This paper presents the formation of novel NLO network polyurethane and investigates polymer structure from infrared spectra, density, and thermal analysis data. The effects of poling condition and storage time and thermal annealing on SHG activity are studied in connection with polymer structure.

Experimental Section

Monomers. Figure 1 shows the chemical structure and codes of monomers for novel NLO network polyurethane.

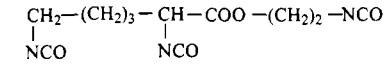

LTI

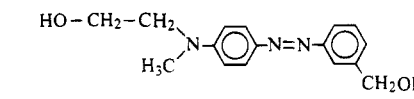

AZODIOL

Figure 1. Chemical structure and codes of monomers used for this study.

Lysine triisocyanate (LTI), supplied from Kyowa Hakkou Co., is used without any purification. 4-[*N*-(2-Hydroxyethyl)-*N*-methylamino]-3′-(hydroxymethyl)azobenzene (AZODIOL) dye is newly synthesized by the diazo-coupling reaction of *N*-(2-hydroxyethyl)-*N*-methylaniline with *m*-aminobenzyl alcohol. *m*-Aminobenzyl alcohol diazonium salt was prepared from *m*-aminobenzyl alcohol (5.90 g, 0.048 mol) with sodium nitrite (3.60 g, 0.052 mol) in an ethanol/water (50/50 by vol %) mixture (40 mL) with 37% hydrochloric acid (12.5 mL) at a temperature of 5 °C for 15 min. Obtained diazonium salt of *m*-aminobenzyl alcohol was coupled with 2-(*N*-methylanilino)ethanol (10.6 g, 0.07 mol) in 5 mL an acetic acid solution at a temperature of around 0 °C for 15 min. Then sodium acetate (3.40 g, 0.041 mol) was added to the reaction mixture, which was then left in an ice bath for 1 h, and another sodium acetate (3.40 g, 0.041 mol) was added to that reaction mixture, which was then left for 30 min. After the temperature was raised to room temperature, a 20% sodium hydroxide solution (5 mL) was added and the whole mixture was left stirring at room temperature for 30 min. Resultant AZODIOL was filtered, washed with water, recrystallized from methanol several times, and dried in an oven. The melting point of AZODIOL measured by DSC is 112.7 °C. Elemental analysis gives the composition ratio: C, 67.27; H, 6.68; O, 11.29; N, 14.77; which can be compared with the calculated one: C, 67.34; H, 6.71; O, 11.21; N, 14.73. Figure 2 shows the ^{1}H-NMR spectrum of AZODIOL measured at 20 °C in acetone-*d*.

Preparation of Prepolymers. Since the isocyanate group was very sensitive to moisture in the air, LTI was preserved in a vial with a screw cap in a nitrogen atmosphere. LTI (62.5 mg, 0.234 mmol) and AZODIOL (100 mg, 0.351 mmol) dis-

* To whom all correspondence should be addressed.

® Abstract published in *Advance ACS Abstracts,* August 15, 1995.

0024-9297/95/2228-6437$09.00/0

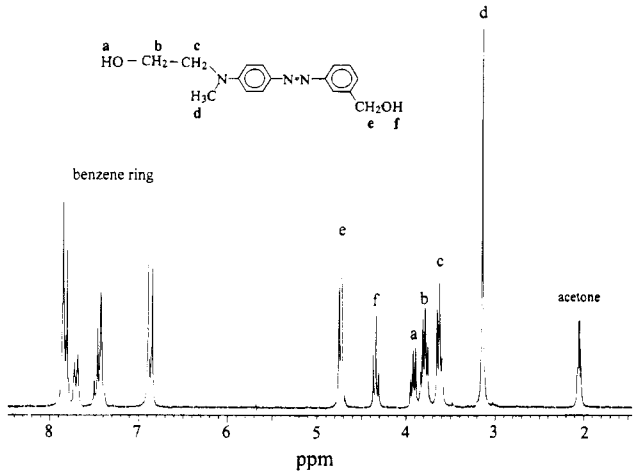

Figure 2. ^{1}H-NMR spectrum of AZODIOL.

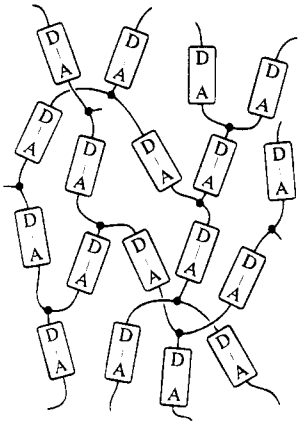

Figure 3. Schematics of aligned NLO-phore in the simultaneous network formation.

solved in distilled dimethylacetamide was heated at 85 °C for 3 min to form prepolymer. The gelation occurs for the time above 5 min at the same condition. The prepolymer obtained was spun-cast on an indium tin oxide (ITO) coated glass substrate. After the spun-cast films were dried in vacuo for 24 h at room temperature, they were subjected to the successive *in-situ* poling and network formation. The thickness of the film is in the range of submicrons.

***In-Situ* Poling and Simultaneous Network Formation.** The corona poling technique was employed to orient NLO-phore to the poling direction. The distance between 0.1-ϕ tungsten wire for corona poling and the sample was kept at 1.4 cm.

Two types of *in-situ* poling and simultaneous network formation were employed. One is the one-step poling process: while high voltage between 5.0 and 8.0 kV was applied to a corona wire, the sample film was heated up to a given temperature between 70 and 190 °C, held at that temperature for 10 min, and then cooled down to room temperature for 40 min. In this poling process, a poling time longer than 10 min causes the film surface to be opaque. Another is the two-step poling process: while high voltage was applied to a corona wire, the sample was heated up and held at 90 °C for 1 h, then heated up again to a given temperature between 90 and 190 °C, and held at that temperature for 30 min. Then the sample was cooled down to room temperature while applying the poling field.

Figure 3 illustrates the schematic picture of an aligned NLO-phore by poling in the polyurethane network.

SHG Measurements. The SHG was measured by the Maker fringe method.[10,11] The laser source is a Continuum Model Surelite-10 Q-switched Nd:YAG pulse laser with 1064-nm p-polarized fundamental beam (320 mJ maximum energy, 7 ns pulse width, and 10 Hz repeating rate). A generated second harmonic (SH) wave is detected by a Hamamatsu Model R928 photomultiplier. The SH signal averaged on a Stanford Research Systems (SRS) Model SR-250 gated integrator and boxcar averager module is transferred to a microcomputer through a SRS Model SR-245 computer interface module. The detailed experimental procedure is described in refs 12 and 13.

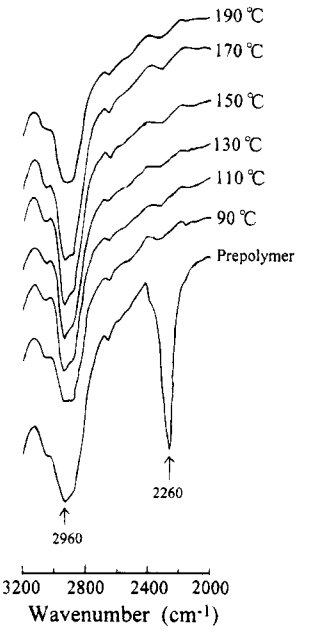

Figure 4. IR spectra of prepolymer film and the sample films postpolymerized at fixed temperatures for 1 h. Temperatures are shown in the figure.

Characterization. Ultraviolet–visible spectra of the films are measured on a Shimadzu Model UV-2101PC spectrophotometer controlled by a PC microcomputer. m-Line method was employed to measure the refractive indices of materials using a prism coupling apparatus. Laser sources are a polarized He–Ne laser (632.8 nm) and a polarized laser diode (830 nm). The prism of TaFD21 (HOYA Glass) with a high refractive index (1.92588 at 632.8 nm) and a spin-coated or cast film was coupled with a matching fluid of diiode methane. Guided-wave spectra (m-lines) were obtained to determine the refractive indices.

The nuclear magnetic resonance (NMR) spectrum was measured with TMS as an internal standard at 20 °C using a Varian Model Gemini-200. The infrared (IR) spectrum was recorded on a Jasco A-1 spectrophotometer using a thin film on a KRS substrate. Differential scanning calorimetry (DSC) is carried out at a heating rate of 10 °C/min in a nitrogen atmosphere, using a Perkin-Elmer DSC7 controlled by a 1020 TA workstation. Thermomechanical analysis (TMA) was performed in a penetration mode under a pressure of 10 kg/cm^2 and a heating rate of 10 °C/min in a nitrogen atmosphere, using a Seiko Instruments Model TMA 100 thermomechanical analyzer controlled by a SSC-5200 disc station. Thermogravimetry (TG) was performed with a Shimadzu Model DT-30 thermogravimetric analyzer at a heating rate of 10 °C/min in a nitrogen atmosphere.

The density of the polymer film was measured using a sink and float test in a mixture of heptane and tetrachloromethane at 30 °C.

Results and Discussion

Network Formation. Figure 4 shows the IR spectra of prepolymer film and the sample films subjected to the heat treatment at the fixed temperatures for 1 h which are shown in the figure. Absorption peaks at wavenumber of 2260 and 2960 cm^{-1} are ascribed to diisocyanate and methylene groups, respectively. Heat treatment causes the large decrease of the absorption peak due to the diisocyanate group at the wavenumber of 2260 cm^{-1}, while it does not affect the absorption

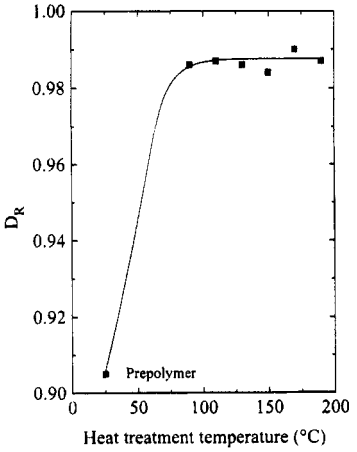

Figure 5. Plot of the degree of reaction against temperature for postpolymerization.

Table 1. Absorption Ratio, A_{2260}/A_{2960}, and Concentration Ratio, [NCO]/[CH_2], of Isocyanate and Methylene Groups for a Known Aliphatic Isocyanate Compound

sample	[NCO]/[CH_2]	A_{2260}/A_{2960}
n-propyl isocyanate	0.5	6.91
butyl isocyanate	0.333	4.53
n-octadecyl isocyanate	0.058	1.16

intensity due to the methylene group around the wavenumber of 2960 cm^{-1}. These IR data provide the estimation of the degree of reaction as we did for other network polymers.[14] The degree of reaction, D_R, can be calculated as

$$D_R = X/3 \tag{1}$$

where

$$\frac{[NCO]}{[CH_2]} = \frac{3 - X}{9}$$

is the number of isocyanate groups reacted to form a urethane linkage. The concentration ratio of [NCO]/[CH_2] was estimated from the ratio in IR absorbance due to isocyanate and methyl groups at wavenumbers of 2260 and 2960 cm^{-1}. In order to get a quantitative ratio of [NCO]/[CH_2], the calibration curve between A_{2260}/A_{2960} and [NCO]/[CH_2] made by the known isocyanate compounds as shown in Table 1 was used.

Figure 5 shows the plot of the degree of reaction against the heat treatment temperature. The fact that D_R is 90% for prepolymer shows that the network formation proceeds during the film cast process at room temperature for 24 h in vacuo. Heat treatment at higher temperature provides the completion of network formation.

Polymer Structure. As described in the Experimental Section, two types of poling processes including heat treatment have been employed to achieve the preferable orientation of NLO-phore. Therefore, it is important to investigate the effect of the heat treatment on polymer structure. The sample films should be subjected to the same heat treatment condition as they are poled. The plots in Figures 6 and 8 were measured for the samples subjected to the same heat treatment condition as they are poled. Thus one- and two-step poling in Figures 6 and 8 are used as the meaning of one- and two-step heat treatment.

The dependence of density on the heat treatment temperature is plotted for both one- and two-step poling processes in Figure 6. As shown in Figure 4, more than 98% isocyanate group has reacted at a temperature of 90 °C. Thus, the significant increase of density at a temperature above 170 °C is attributed to further cross-linking by cleavage (or decomposition) of diazo linkage at higher temperature. Weight loss measurement by TG supports the thermal decomposition of polymer film at a temperature above 170 °C as shown in Figure 7. It is noted that the density for the sample prepared by the two-step poling process is larger than that prepared by one-step poling process. This result implies that the longer time of heat treatment in the two-step poling process causes the increase of the cross-linking density and thus the decrease of free volume.

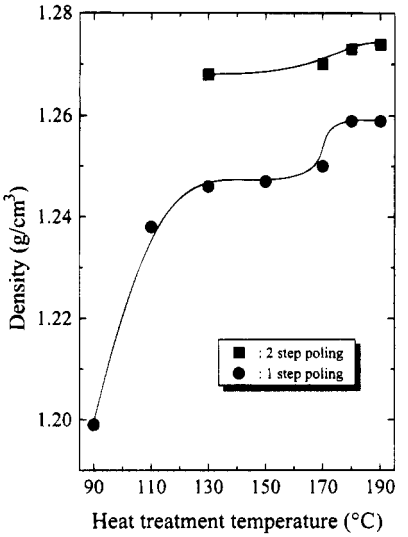

Figure 6. Dependence of density on postpolymerization temperature.

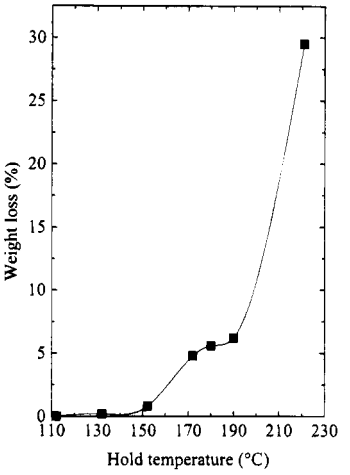

Figure 7. Weight loss by TG for the samples held at various temperatures, which are shown on the horizontal axis of the figure, for 1 h.

Network polymer films of interest did not show any evidence of crystallization and crystal structure from the measurements of thermal analysis of DSC and wide-angle X-ray scattering. DSC and TMA measurements provide the transition temperature due to the transition from the glassy to rubbery state. A plot of T_g against heat treatment temperature is shown in Figure 8. T_g increases with increasing heat treatment temperature.

The difference of microstructure such as free volume may relate to SHG activity for the sample, which will be discussed below in connection with the long-term thermal stability of SHG activity.

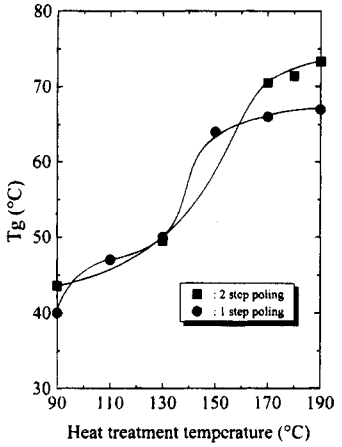

Figure 8. Plot of T_g values versus postpolymerization temperature.

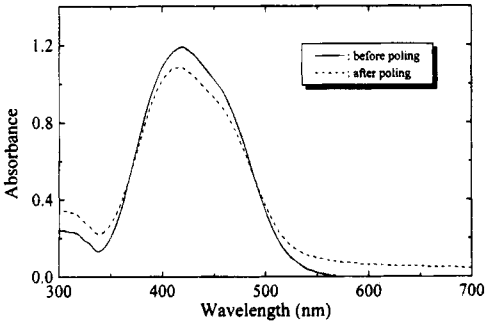

Figure 9. Absorption spectra of polymers before and after poling.

Absorption Spectra. Figure 9 shows absorption spectra of polymers before and after poling. Poling causes a decrease of the absorption intensity and a shorter wavelength shift of the absorption peak. Heat treatment itself at the same conditions of temperature and time as the sample film is poled does not cause the change of intensity and spectral shift. Thus, the intensity change is ascribed to the orientation of the azobenzene dye to the direction of the film thickness induced by poling. The spectral blue shift has been reported for other cross-linked main-chain polymers,[5] which is in contrast to the red shift observed in most side-chain polymers.[15]

Refractive Indices and Determination of SHG Coefficients. The refractive indices (RI) for the transverse electric field (TE) mode are measured using the m-line method. The resultant RI's of unpoled polymer films were 1.696 and 1.649 at wavelengths of 632.8 and 830 nm, respectively.

Wavelength dispersion of RI can be fitted to a one-oscillator Sellmeier-dispersion formula,

$$n_f^2(\lambda) - 1 = \frac{q}{1/\lambda_0^2 - 1/\lambda^2} + A \qquad (2)$$

where λ_0 is the absorption wavelength of the dominant oscillator, q is a measure for the oscillator strength, and A is a constant containing the sum of all the other oscillators. Figure 10 shows the plot of RI at wavelengths of 632.8 and 830 nm and the predicted curve of the wavelength dispersion of RI using eq 2. RI values of 1.64 at 1064 nm and 1.78 at 532 nm for the SHG calculation are obtained from the predicted curve in the figure.

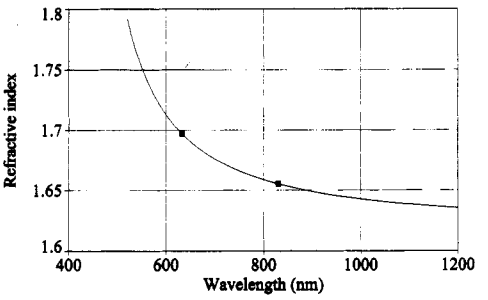

Figure 10. Plot of RI at wavelengths of 632.8 and 830 nm and the predicted plot curve (solid curve) of the wavelength dispersion of RI using eq 2.

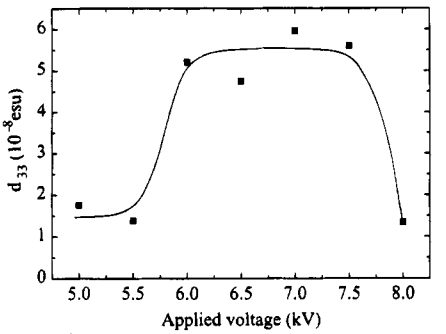

Figure 11. Plot of d_{33} values when the applied corona voltage varies from 5.0 to 8.0 kV.

Table 2. Surface State of Spun-Cast Film after Poling at Various Applied Voltages from 5.0 to 8.0 kV and the Possibility of SHG Activity Measurement at Poling just Below the Corona Wire

applied voltage (kV)	surface state	possibility of SHG measurement at point just below corona wire
5.0	transparent	possible
5.5	transparent	possible
6.0	almost transparent	possible
6.5	semi-transparent	partly possible
7.0	semi-transparent	impossible
7.5	semi-transparent	impossible
8.0	opaque	impossible

The SHG coefficients of the polymers are made relative to a Y-cut quartz plate ($d_{11} = 1.2 \times 10^{-9}$ esu). The typical Maker fringe patterns were observed for both the cases of a p-polarized and an s-polarized fundamental beam.

Optimum Poling Condition for SHG. It is important to determine the optimum poling condition (corona voltage and poling temperature) to obtain better SHG activities. Figure 11 shows the change of the SHG coefficient of d_{33} when the applied corona voltage was varied from 5.0 to 8.0 kV. A one-step poling process was employed. At the voltage below 4.5 kV, no SHG activity was obtained. Table 2 summarizes visual observation of the surface state of the sample and the possibility of the SHG measurement of the sample film at the point just below the corona wire. At the applied corona voltage above 6.5 kV, the film surface became semi-transparent or opaque and it became impossible to measure the SHG activity of the sample film at the point just below the corona wire. As shown in Figure 11, the applied voltage between 6.0 and 6.5 kV is the optimum poling voltage.

Comparison of One-Step and Two-Step Poling Processes for SHG Activity. The dependence of SHG activity on the poling temperature is shown for one-step and two-step poling processes in Figure 12. The opti-

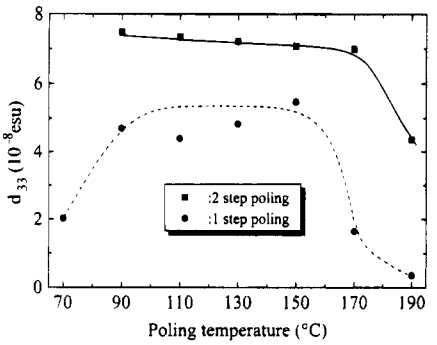

Figure 12. Dependence of SHG activity on the poling temperature for one-step and two-step poling processes.

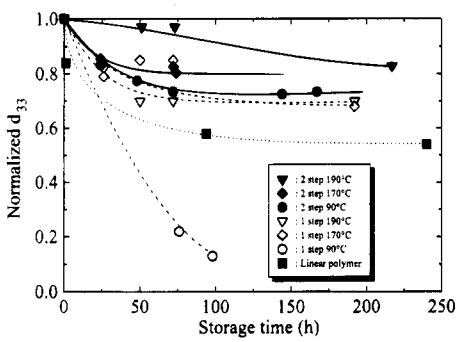

Figure 13. Long-term thermal stability of d_{33} for one-step and two-step poling processes.

mum poling temperature ranges from 90 to 150 °C for the one-step poling process, while it ranges from 90 to 170 °C for the two-step poling process. The d_{33} value for two-step poling process is larger than that for the one-step poling process. The large decrease of SHG activity at the temperature of 190 °C is ascribed to the thermal decomposition of the azobenzene chromophore, which is supported by the weight loss of sample at that temperature by TG measurement as shown in Figure 7.

Figure 13 shows the long-term thermal stability of d_{33} for both one-step and two-step poling processes. The vertical axis indicates the d_{33} values normalized by that measured at time = 0, $d_{33}(h)/d_{33}(0)$. Temperatures inset are those for poling and simultaneous network formation. The long-term thermal stability is measured at room temperature. The higher poling temperature gave rise to the higher thermal stability of SHG activity for both poling processes. It is clear that the long-term thermal stability of SHG activity for the sample prepared by the two-step poling process is better than that by the one-step poling process. As shown in Figure 6, the density for the sample prepared by the two-step poling process is higher than that prepared by the one-step poling process. The density result implies that the sample prepared by the two-step poling process has a smaller free volume than that prepared by the one-step poling process. Thus, the better thermal stability of SHG activity for the sample prepared by the two-step poling process is ascribed to the smaller free volume of the sample. SHG activity of the linear polyurethane of AZODIOL with 4,4′-diphenylmethane diisocyanate with a T_g of 67 °C is plotted against the storage time in the same figure. The thermal stability of network polymers is better than that of the linear polymer. The better thermal stability of SHG activity of network polymer is ascribed to the suppression of local molecular motion due to three-dimensional cross-linkage formation. However, SHG activity of either sample has been decayed

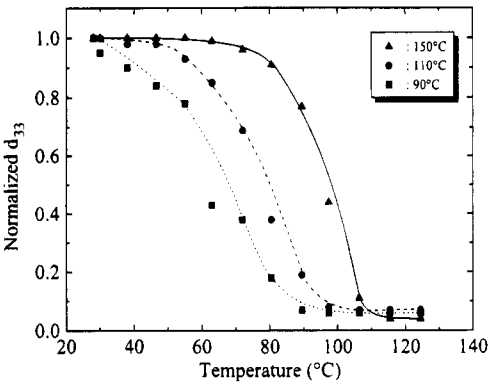

Figure 14. Temperature profiles of d_{33} for samples poled at various temperatures of 90, 110, and 150 °C. SHG measurement was carried out at the higher fixed temperature shown on the horizontal axis in the figure.

for several days and then seems to be leveled out, even if these measurements were carried out at a temperature below T_g. These fast-relaxation components may be due to the local relaxation of oriented NLO-phore. Another possibility is that these fast-relaxation components may be due to the release of the injected surface charges which creates the local space charge field that temporarily stabilizes the orientation of NLO-phore.

SHG activity measurement is carried out at 30 °C and then at higher fixed temperature for the sample films poled at temperatures of 90, 110, and 150 °C. The results are plotted in Figure 14 in the form of SHG coefficients d_{33} normalized by that measured at 30 °C (vertical axis) against measurement temperature (horizontal axis). Significant SHG loss starts at temperatures around 80, 50, and 30 °C (initial SHG loss temperature) for the samples poled at temperatures of 150, 110, and 90 °C, respectively. The initial SHG loss temperature is close to the glass transition temperature of each sample which is shown in Figure 8. For each sample, the large activity loss of SHG occurs at temperatures above 20−30 °C of the initial SHG loss temperature. Thus these SHG losses can be related to the reorientation of NLO-phore due to the thermal relaxation of polymer chain at a temperature above T_g.

Conclusion

Novel network polyurethane of trifunctional isocyanate monomer of LTI with NLO diol monomer of AZODIOL has been prepared for thermally stable NLO materials. Two types of poling processes were employed to get a preferable orientation of NLO-phore in the network polyurethane. Better long-term thermal stability of SHG can be obtained for the sample prepared by the two-step poling process. This better thermal stability is interpreted to be due to the smaller free volume for that polymer.

Acknowledgment. We thank Prof. Minoru Nagata, Kyoto Pref. University, for discussing the monomer synthesis.

References and Notes

(1) Eich, M.; Sen, A.; Looser, H.; Bjorklund, G. C.; Swalen, J. D.; Twieg, R.; Yoon, D. Y. *J. Appl. Phys.* **1989**, *66*, 2559.
(2) Eich, M.; Reck, B.; Yoon, D. Y.; Willson, C. G.; Bjorklund, G. C. *J. Appl. Phys.* **1989**, *66*, 3241.
(3) Papers presented in *Organic Materials for Non-linear Optics II*; Hann, R. A.; Bloor, D., Eds.; The Royal Society of Chemistry: Cambridge, U.K., 1991.

(4) Jungbauer, D.; Reck, B.; Twieg, R.; Yoon, D. Y.; Willson, C. G.; Swalen, J. D. *Appl. Phys. Lett.* **1990**, *56*, 2610.
(5) Ranon, P. M.; Shi, Y., Steier, W. H.; Xu, C.; Wu, B.; Dalton, L. R. *Appl. Phys. Lett.* **1993**, *62*, 2605.
(6) Boogers, J. A. F.; Klaase, P. Th. A.; de Vliger, J. J.; Tinnemans, A. A. *Macromolecules* **1994**, *27*, 205.
(7) Stähelin, M.; Burland, D. M.; Ebert, M.; Miller, R. D.; Smith, B. A.; Twieg, R. J.; Volksen, W.; Walsh, C. A. *Appl. Phys. Lett.* **1992**, *61*, 1626.
(8) White, K. M.; Francis, C. V.; Isackson, A. J. *Macromolecules* **1994**, *27*, 3619.
(9) (a) White, K. M.; Cross, E. M. *J. Appl. Phys.* **1995**, *77*, 833. (b) Cross, E. M.; White, K. M.; Moshrefzadeh, R. S.; Francis, C. F. *Macromolecules* **1995**, *28*, 2526.
(10) Maker, P. D.; Terhune, R. W.; Nisenoff, M.; Savage, C. M. *Phys. Rev. Lett.* **1962**, *8*, 21.
(11) Jerphagnon J.; Kurtz, S. K. *J. Appl. Phys.* **1970**, *40*, 1667.
(12) Tsutsumi, N.; Ono, T.; Kiyotsukuri, T. *Macromolecules* **1993**, *26*, 5447.
(13) Tsutsumi, N.; Fujii, I.; Ueda, Y.; Kiyotsukuri, T. *Macromolecules* **1995**, 28, 950.
(14) Tsutsumi, N.; Chen, Y.; Kiyotsukuri, T. *J. Polym. Sci., Part A: Polym. Chem.* **1991**, *29*, 1963.
(15) Page, R. H.; Jurich, M. C.; Reck, B.; Sen, A.; Twieg, R. J.; Swalen, J. D.; Bjorklund, G. C.; Willson, C. G. *J. Opt. Soc. Am. B* **1990**, *7*, 1239.

MA950320G